

# Mutations at Position −10 in the $\lambda$ $P_R$ Promoter Primarily Affect Conversion of the Initial Closed Complex ( $RP_c$ ) to a Stable, Closed Intermediate ( $RP_i$ )

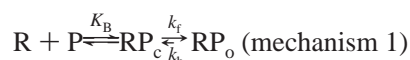
Melissa McKane, Cheryl Malone, and Gary N. Gussin\*

Department of Biological Sciences, University of Iowa, Iowa City, Iowa 52246 USA

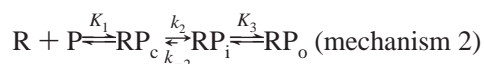
Received August 11, 2000; Revised Manuscript Received December 12, 2000

**ABSTRACT:** The effects of mutations of −10 T:A to A:T, C:G, or G:C in the  $\lambda$   $P_R$  promoter on formation of transcriptionally competent open complexes were studied by DNase I footprinting,  $KMnO_4$ -sensitivity, and abortive initiation kinetic analysis. The mutations −10A (T:A → A:T) and −10C significantly reduce  $k_f$ , the composite rate constant for conversion of closed complexes ( $RP_c$ ) to open complexes ( $RP_o$ ) but do not affect  $K_B$ , the equilibrium constant for formation of closed complexes. Unlike the other mutants or wild-type  $P_R$ , the mutation with the largest effect on open complex formation, −10G (T:A → G:C), substantially decreases the occupancy of the promoter. When reduced occupancy is taken into account, the calculated effect of the mutation on  $k_f$  is a 20-fold reduction. Analysis of open complex formation by a three-step pathway that includes an additional intermediate,  $RP_i$ , indicates that the primary effect of all three mutations is a reduction in the rate of isomerization of  $RP_c$  to  $RP_i$ , which precedes DNA strand separation. Thus, RNA polymerase holoenzyme must recognize specific base pairs in the −10 region of  $P_R$  while the DNA is still double-stranded. Comparison of the observed level of stable complexes ( $RP_i$  plus  $RP_o$ ) with the level of productive complexes ( $RP_o$ ) indicates that the −10G mutation may also affect the equilibrium between  $RP_i$  and  $RP_o$  at 37°. Open complexes formed at the three mutant promoters are approximately 3–5 times less stable at 37° than those formed at wild-type  $P_R$ .

Open complex formation by eubacterial RNA polymerase holoenzyme (RNAP)<sup>1</sup> can be characterized minimally by a simplified, two-step pathway (mechanism 1), in which RNAP and promoter DNA form a specific *closed* complex,  $RP_i$ , which isomerizes to the *open* complex,  $RP_o$  (1):



During isomerization, DNA strands separate to permit base pairing between substrate NTPs and the template strand (1–3). The dependence of open complex formation at  $\lambda$   $P_R$  (4, 5) and *lacP*<sub>UV5</sub> (6) on temperature and salt implicated at least one additional intermediate,  $RP_i$  (mechanism 2):



Step 2 is thought to involve an isomerization of RNAP that “nucleates” strand separation (2, 3, 7).  $RP_i$ , which is equivalent to  $I_2$  in other formulations of the same mechanism (3), has properties common to both open and closed complexes. The DNA strands in the complex are not yet separated (3), but because the second step is irreversible,  $k_2$  is a component of  $k_f$  in mechanism 1. In addition, like  $RP_o$ ,  $RP_i$  is resistant to polyanions (6).

We examined the effects of mutations at a single site (−10) in the  $\lambda$   $P_R$  promoter on kinetic parameters associated with each of the three steps in mechanism 2, one goal being to determine whether particular mutations in the −10 consensus region affect DNA strand separation per se. The latter question is of particular interest since RNAP recognizes specific −10 consensus nucleotides only in the non-template DNA strand when it initiates transcription on templates containing preformed heteroduplexes spanning the −10 region (8). In addition, the holoenzyme binds sequence-specifically to single-stranded DNA containing the −10 consensus sequence (9).

At 37 °C, mutation of the T:A base pair at −10 to G:C has the strongest effect on open complex formation, while mutations to A:T and C:G have much less severe effects. The mutant phenotypes correlate well with the in vivo effects of the corresponding mutations in the P22 *ant* promoter (10). At 20 °C, values of  $K_3$  obtained from temperature-shift experiments for the mutant promoters were not significantly different from those obtained for wild-type  $P_R$ . On the basis of an analysis of the rate of equilibration of  $RP_i$  and  $RP_o$  after the temperature shift, we conclude that neither the 3- to 4-fold effects of the −10A (T:A → A:T) and −10C mutations on  $k_f$  at 37 °C nor the 20-fold effect of −10G can be explained by a change in  $K_3$ . These results indicate that at least some interactions between specific nucleotides in the −10 region and RNAP take place prior to strand separation. Furthermore, our data demonstrate that −10C, a mutation from T:A to C:G, which should stabilize the DNA double-helix in the region in which strand separation occurs, does not significantly inhibit strand separation per se.

\* To whom correspondence should be addressed. Telephone: 319-335-1113; FAX: 319-335-1069.

<sup>1</sup> Abbreviations: bp, base pair(s); CpA, cytidyl-(3′ → 5′)-adenosine; Glu, glutamate; NTP, ribonucleoside triphosphate; RNAP (RNA polymerase holoenzyme);  $RP_o$ ,  $RP_c$ , and  $RP_i$ , RNA polymerase–promoter open, closed, and intermediate complex, respectively.

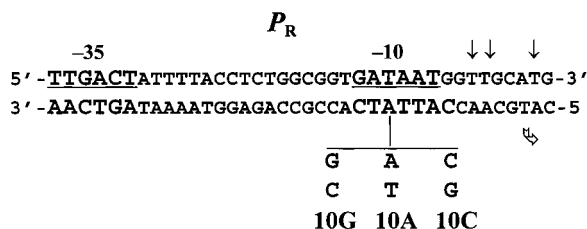


FIGURE 1: Nucleotide sequence of  $P_R$ . Sequences corresponding to the -10 and -35 consensus sequences (5'-TATAAT-3' and 5'-TTGACA-3', respectively) are underlined. Nucleotide sequence changes are indicated for the -10 mutations used in this study. Vertical arrows at -4, -3, and +2 indicate cleavage sites for  $\text{KMnO}_4$ . The open arrow denotes the transcription start site. The KM11 mutation in  $P_{RM}$  (12), which is present on all templates, is located at -72 with respect to  $P_R$ .

## EXPERIMENTAL PROCEDURES

**Plasmids and DNA Fragments.** Bacteriophage Mt101 contains a phage  $\lambda$  678-bp *EcoRI*–*HindIII* DNA fragment inserted between *EcoRI* and *HindIII* sites in the polylinker of a derivative of M13mp18 (11). Oligonucleotide-directed mutagenesis of Mt101 was used to generate the mutants used in this study. DNA fragments used as templates for RNAP were obtained from plasmids containing  $P_{RM}$  and  $P_R$ , which were constructed by inserting 372-bp *EcoRI*–*NsiI* fragments from Mt101 derivatives into pSW305 (11). All templates also contained the mutation KM11, which inactivates  $P_{RM}$  (12).

**Determination of Kinetic Parameters.** To determine  $K_B$  and  $k_f$  (1, 13), DNA (0.05–1.0 nM) and RNAP were combined in transcription buffer [40 mM Tris-HCl, pH 8.0, 0.1 M potassium glutamate (KGlu), 10 mM  $\text{MgCl}_2$ , 1 mM dithiothreitol, and 100  $\mu\text{g}/\text{mL}$  of bovine serum albumin] plus 0.5 mM CpA and 50  $\mu\text{M}$   $\alpha$ -[ $^{32}\text{P}$ ]-UTP (spec. act. 0.4–0.8 Ci/mmol). Samples were analyzed as described previously (14) and the data were fit to eq 1 (13):

$$\tau_{\text{obs}} = 1/k_f + 1/K_B k_f [\text{RNAP}] \quad (1)$$

Rates of dissociation ( $k_d$ ) of preformed complexes were measured in the presence of 30  $\mu\text{g}/\text{mL}$  of heparin as described previously (14) using abortive initiation or gel mobility shift assays to measure dissociation at 37 or 20°, respectively.

Determination of  $K_3$  was based on the method devised by Buc and McClure (6), except that open complexes were assayed by probing for sensitivity to  $\text{KMnO}_4$  following a shift of preformed open complexes from 37 to 20 °C, as described previously (14). Data obtained after the temperature-shift were fit to a rearranged version of eq 1 of Buc and McClure (6), in which  $f$  is the fraction of open complexes remaining as a function of time after the temperature downshift:

$$f = [e^{-\beta t} + K_3]/(1 + K_3) \quad (2)$$

**DNase I Footprinting.** *EcoRI*-digested pSW305 derivatives were labeled at their 3' ends by incubating the DNA with the Klenow fragment of DNA polymerase I in the presence of [ $\alpha$ - $^{32}\text{P}$ ]-dATP followed by incubation with unlabeled dATP. Following digestion of the radioactive DNA by *HindIII*, the products were separated by polyacrylamide gel electrophoresis and the isolated 367-bp *EcoRI*–*HindIII* fragment, labeled on the  $\lambda$  I strand (top strand in Figure 1),

was purified by elution from an Elutip column (Schleicher and Schuell, Keene, NH). To assay binding by RNA polymerase, prewarmed DNA (final concentration, 1 nM) and RNAP (final concentration, 20 nM active enzyme) were incubated in transcription buffer. At indicated times, 15  $\mu\text{L}$  aliquots were taken and treated with 5  $\mu\text{L}$  of DNase I (2  $\mu\text{g}/\text{mL}$  at 20 °C or 0.5  $\mu\text{g}/\text{mL}$  at 37 °C) in 10 mM Tris-HCl, pH 8.0, 5 mM  $\text{MgCl}_2$ , 1 mM  $\text{CaCl}_2$ , 2 mM DTT, and 0.1 M KCl for 1 min. Reactions were stopped by addition of one volume of formamide stop buffer (98% formamide, 10 mM EDTA, pH 8.0, 1 mg/mL xylene cyanol, 1 mg/mL bromophenol blue). Products were separated by electrophoresis on a 7 M urea/8% polyacrylamide gel and analyzed on a Molecular Dynamics phosphorimager. Fractional occupancy at each time point was determined by (i) subtracting background intensities from intensities of selected bands in two protected regions (near -35 and +1) and an unprotected region (near -60), which are boxed in Figure 2; (ii) calculating the ratio of intensities (after subtracting background) in selected bands in the protected region to the intensities in the absence of RNAP; and (iii) normalizing with a respect to the corresponding ratios for reference bands in the unprotected region. Fractional occupancies based on intensities of the bands at -35 (see Figure 2) or +1 were within 10% of each other in almost all cases and were averaged to yield the data in Table 1. Positions of the bands in the gel were determined by comparison with partial sequencing ladders and with previous footprints obtained in our laboratory (11) and the Record laboratory (3).

**$\text{KMnO}_4$ -Sensitivity.** DNA (final concentration 1 nM, labeled and purified as described for DNase I footprinting) and RNAP (final concentration, 20 nM, active enzyme) were prewarmed, mixed, and incubated at 20 or 37 °C in transcription buffer without DTT. Samples (40  $\mu\text{L}$ ) were taken and added to 1.1  $\mu\text{L}$  of  $\text{KMnO}_4$  (14.8 mM) for 1 min. Reactions were stopped by addition of 10  $\mu\text{L}$  of stop mix (3.5 M  $\beta$ -mercaptoethanol, 1.4 M NaOAc). Reference DNA (2  $\mu\text{L}$  of the original labeled 367-bp fragment, digested by *HincII* to generate a 137-bp labeled fragment) was added, followed by phenol extraction and two cycles of ethanol precipitation. Pelleted DNA was resuspended in 150  $\mu\text{L}$  of piperidine (1/10 dilution), incubated at 90 °C for 30 min, precipitated with ethanol, and then resuspended in formamide dye buffer. Following electrophoresis on a 7 M urea/8% polyacrylamide gel, the products were quantified using a Molecular Dynamics phosphorimager.

**Enzymes and Materials.** RNAP holoenzyme was purchased from Epicenter (Madison, WI) or purified by the method of Burgess and Jendrisak (15) as modified by Lowe et al. (16). The fraction of active enzyme was determined by titration of DNA containing only the  $\lambda$  late promoter  $P_R$  (17). Restriction enzymes, T4 DNA ligase, and Klenow fragment were purchased from New England Biolabs (Beverly, MA) and Promega (Madison, WI). CpA was obtained from ICN Biomedicals (Irvine, CA). DNase I was purchased from Sigma Chem. Co. (St. Louis, MO). Radioactive substrates were obtained from Amersham/Searle (Arlington Heights, IL).

## RESULTS

**Formation of Open Complexes at 37 and 20 °C.** The goal of this research was to analyze the effects of mutations at

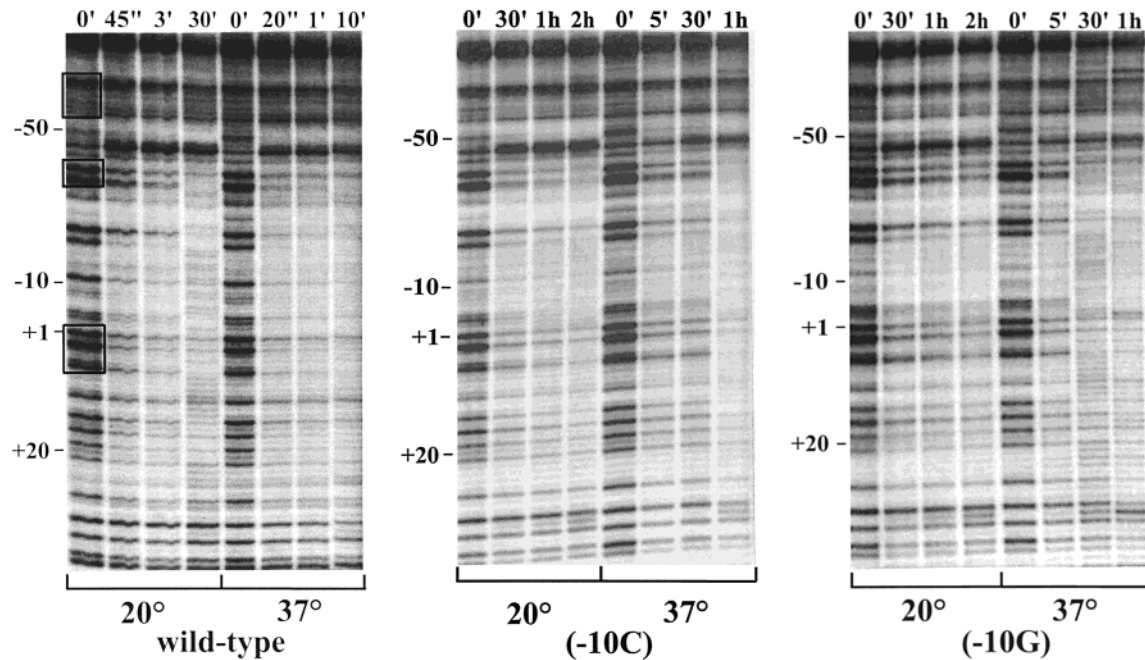


FIGURE 2: DNase I footprints at wild-type and mutant derivatives of  $P_R$ . Samples were withdrawn at the indicated times and treated with DNase I as outlined in Experimental Procedures. The region protected from DNase I digestion extends approximately from +20 to -45 on the  $\lambda$  I strand (top strand in Figure 1). DNA templates used in the left (wild-type), center (-10C), and right (-10G) panels are indicated. Regions used in calculating fractional occupancy are indicated by boxes in the zero time sample for wild-type  $P_R$  at 20°. The upper, middle, and lower boxes enclose an unprotected region near -60, bands at -34, -35, and -37, and bands at +1, +3, and +8, respectively. Positions of bands were determined by comparison with a partial DNA sequence ladder and with previously published footprints of wild-type  $P_R$  (3, 11).

Table 1: Occupancy<sup>a</sup> of  $P_R$  on Mutant and Wild-Type Templates

DNA template	temp (°C)	DNase I footprinting			KMnO <sub>4</sub> -sensitivity	
		occupancy at 30 min (%)	plateau level (%)	time achieved (min) <sup>d</sup>	plateau level (%)	time achieved (min) <sup>d</sup>
$P_R$ wild-type	37	nt <sup>b</sup>	98 ± 2	~1	≅100 <sup>a</sup>	~1
$P_R$ (-10C)	37	76 ± 13	89 ± 2	30–60	84 ± 12	~30
$P_R$ (-10G)	37	53 ± 10	75 ± 9	~30	66 ± 14	~30
$P_R$ wild-type	20	98 ± 6	96 ± 5	3–30	64 ± 4	10–40
$P_R$ (-10C)	20	65 ± 2	85 ± 2	60–120	55 ± 3	60–120
$P_R$ (-10G)	20	50 ± 2	61 ± 5	~120	>27 ± 2 <sup>c</sup>	>120

<sup>a</sup> For DNase I footprinting, occupancy was determined by comparing the intensity of bands in the protected region of the gel to the intensity of bands in the unprotected region. For permanganate sensitivity, occupancy is defined as the intensity of the band corresponding to cleavage at -3, relative to the intensity of the same band on the wild-type template at 37 °C. Percentages are averages of two experiments ± range for the permanganate experiments and averages of three or more experiments ± SD for the DNase I footprinting experiments. <sup>b</sup> nt, not tested; no 30-min sample was taken because maximal occupancy was attained in less than 10 min. <sup>c</sup> Plateau not attained by 120 min. <sup>d</sup> Indicated times are the estimated times at which maximal occupancy was achieved based on quantitative analysis of phosphorimager data obtained at the time points indicated in Figures 2 and 3.

-10 of  $P_R$  kinetically and determine whether any of the mutations directly affected the strand separation step in the three-step pathway to the open complex (mechanism 2). We focused on mutations at -10, because it is close to the site at which strand separation is initiated (18). To explore the effects of the mutations qualitatively, the ability of RNAP to form a DNase I footprint on the mutant and wild-type templates was assayed in standard transcription buffer containing 0.1 M KCl. Although RNAP at  $P_{RM}$  does not interfere with open complex formation at wild-type  $P_R$  at 37° (12), we wanted to avoid the possibility that interference

might occur on mutant templates at 37° or on mutant or wild-type templates at 20°. Therefore, all DNA templates contained the mutation KM11 (Figure 1), which inactivates  $P_{RM}$ . The protected regions (Figure 2) for wild-type and the two mutant promoters are not significantly different from each other, nor do they differ significantly from previous footprints for wild-type  $P_R$  obtained in our laboratory (11) or the Record laboratory (3). The protected region extends primarily from -45 to +20, with some protection also observed at about -50. There is no detectable difference between footprints obtained at 20° and those obtained at 37° at any time point. This is expected since at  $P_R$  the footprints for  $RP_i$  and  $RP_o$  are indistinguishable (3).

Although the wild-type T at -10 in the nontemplate (top) strand of  $P_R$  is not so highly conserved as some consensus nucleotides, the mutations -10C and -10G significantly reduce the overall rate of open complex formation. At 37 °C and 20 nM RNAP, it takes about 1 min to achieve maximal occupancy on the wild-type template, while approximately 30 min or longer are required on the mutant templates (Table 1). Furthermore, the mutation -10G decreases the final occupancy of  $P_R$  by about 25%.

In similar experiments, open complexes were assayed by probing the sensitivity of separated DNA strands to KMnO<sub>4</sub>, which induces cleavage at thymidine residues in single-stranded DNA (19). Permanganate sensitivity should be characteristic only of  $RP_o$ , but not  $RP_i$  (3, 20). Because the 3' end of the top strand (Figure 1) is labeled with <sup>32</sup>P, these assays are specific for T's in the top strand, and cleavage of a T closer to the 3' end of the fragment should preclude detection of cleavage of a T closer to the 5' end on the same strand. Bands due to cleavage at thymidine residues at +2, -3, and -4 are the most prominent. Figure 3 illustrates



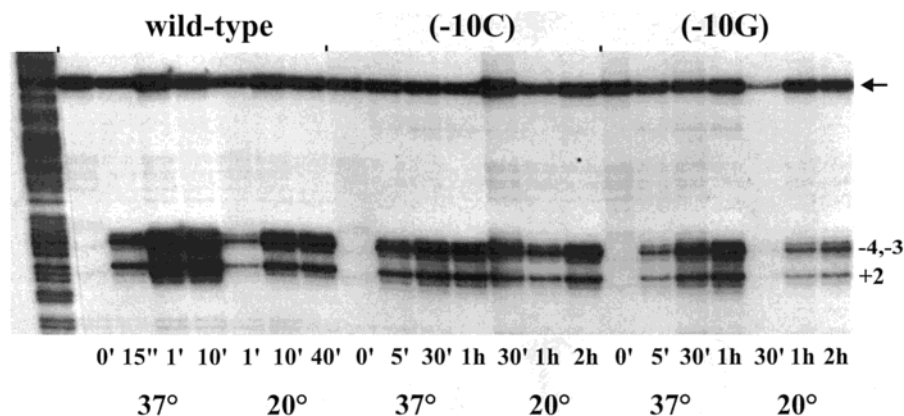


FIGURE 3: Assays of  $\text{KMnO}_4$ -sensitivity of binary complexes as a function of time of incubation at  $37^\circ$ . Open complexes were allowed to form for indicated times at 25 nM RNAP at  $37^\circ$ . Samples were withdrawn at the indicated times and treated with  $\text{KMnO}_4$  as described in Experimental Procedures. Arrows indicate the positions of bands representing cleavage at +2, -3, and -4 as well as the position of reference DNA, which was added to each sample to monitor the recovery of the  $\text{KMnO}_4$ -treated DNA during phenol extraction and electrophoresis. The positions of bands were verified by comparison with a C + T DNA sequencing ladder (leftmost lane).

results of assays of  $\text{KMnO}_4$ -sensitivity as a function of time of incubation of 20 nM RNAP and template DNA at  $37^\circ$  or  $20^\circ$  in buffer containing 0.1 M KCl. Maximal levels of  $\text{KMnO}_4$ -sensitivity of the T at -3 were achieved at approximately the same time that the maximal occupancies were observed in the footprinting experiments (Table 1). At  $37^\circ\text{C}$ , maximal occupancies of wild-type  $P_R$  and the -10C mutant promoter are nearly the same in both the footprinting and permanganate assays, indicating that few, if any, of the stable complexes are  $\text{RP}_i$  (3, 20). However, as measured by  $\text{KMnO}_4$ -sensitivity, the -10G promoter forms only about two-thirds the number of open complexes ( $\text{RP}_o$ ) as wild-type  $P_R$ , and the DNase I footprinting assays (Figure 2) indicate that the mutant promoter forms about three-fourths as many stable complexes ( $\text{RP}_i$  plus  $\text{RP}_o$ ) as the wild-type promoter. Thus, these data suggest that as many as 10–15% of the stable complexes formed at the -10G mutant promoter may be  $\text{RP}_i$ . However, there is substantial variability in plateau levels determined in permanganate sensitivity assays, at least in part because of the lack of an appropriate internal standard for normalization of data obtained with different template DNAs.

For all three templates, the plateau levels at  $20^\circ$  (Table 1) are lower in the permanganate assays than in DNase I footprinting assays, indicating that not all stable complexes are open, i.e., as reported previously (3), some could be  $\text{RP}_i$ .

**Kinetic Analysis of Effects of Mutations at -10 on Open Complex Formation at  $P_R$ .** The footprinting data indicate that the mutations delay formation of strand-separated (open) complexes at both 37 and  $20^\circ\text{C}$  but do not identify the step(s) in the pathway to the open complex that are affected by the mutations. To address this question, abortive initiation lagtime assays (13) were used to determine  $\tau_{\text{obs}}$ , the average time required for open complex formation at several RNAP concentrations for each mutant. These experiments were performed in the presence of 0.1 M potassium glutamate (KGlu) instead of KCl, because the footprinting analysis (Figure 2) indicated that the -10G promoter failed to achieve full occupancy. On the basis of previous studies in which substitution of KGlu for KCl increased final occupancy at wild-type  $P_R$  at  $\geq 0.2$  M salt concentrations (21), we hoped that the substitution would increase the occupancy of the -10G template. This did not prove to be the case, but for

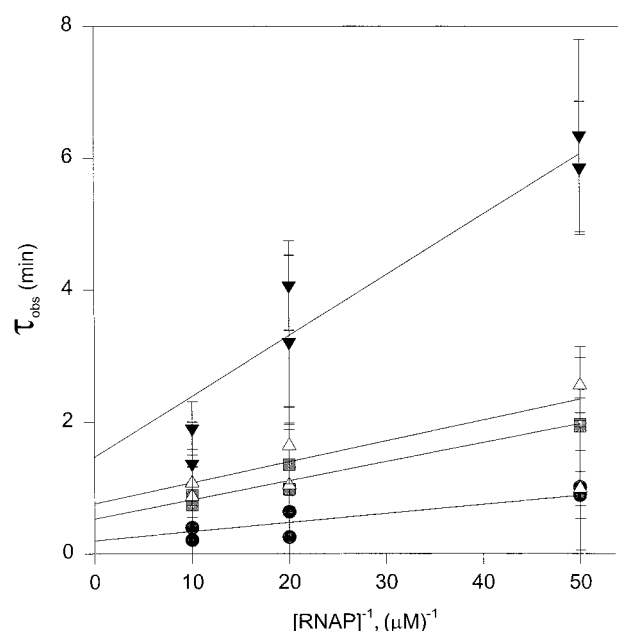


FIGURE 4: Tau plots for wild-type  $P_R$  and -10 mutant promoters. Values of  $\tau_{\text{obs}}$  and standard errors were obtained from lagtime assays (13) of the synthesis of the abortive initiation product CpApU, which corresponds to nucleotides at -1, +1, and +2 of  $P_R$ . Straight lines represent a weighted least squares best fit of the lagtime data to eq 1 (see ref 14). The data for the -10G promoter are not corrected for incomplete occupancy (see text). Symbols: ●, wild-type  $P_R$ ; gray-shaded squares, 10A; △, 10C; ▼, 10G.

consistency, all subsequent kinetic experiments were performed in the presence of KGlu.

Values of  $\tau_{\text{obs}}$  were plotted as a function of  $1/[\text{RNAP}]$  to determine  $K_B$  and  $k_f$  (1, 13) as defined by the two-step mechanism. The time required for open complex formation was greatest for  $P_R$  (-10G) and smallest for wild-type  $P_R$  (Figure 4). Calculated values of  $K_B k_f$  (Table 2) and inspection of Figure 4 indicate that the effects of -10A and -10C on promoter function are virtually identical and are different from the effects of -10G. On the basis of the calculated kinetic parameters, none of the three mutations significantly affects  $K_B$ , but all three mutations decrease  $k_f$ , the rate constant for conversion of  $\text{RP}_c$  to  $\text{RP}_o$ , approximately by factors of 3 (-10C), 4 (-10A), and 8 (-10G).

Table 2: Kinetic Parameters<sup>a</sup> for  $P_R$  Mutants at 37°

$P_R$ allele	$\tau$ (s)	$k_f$ ( $10^{-2} \text{ s}^{-1}$ )	$K_B$ ( $10^6 \text{ M}^{-1}$ )	$K_B k_f$ ( $10^4 \text{ M}^{-1} \text{ s}^{-1}$ )	$k_d$ ( $10^{-5} \text{ s}^{-1}$ )	$K_{eq}$ ( $10^{10} \text{ M}^{-1}$ )
wild-type	11 ± 6	9.0 ± 5.0	13.4 ± 10.3	121 ± 27	0.87 ± 0.08	14 ± 4.4
−10C	32 ± 5	3.1 ± 0.5	18.4 ± 4.8	57 ± 6	3.2 ± 1.6	1.8 ± 1.2
−10A	46 ± 23	2.2 ± 1.1	23.6 ± 20	52 ± 18	4.8 ± 1.3	1.1 ± 0.68
−10G	88 ± 32	1.1 ± 0.4	16.4 ± 8.2	18 ± 3	2.0 ± 0.55	0.9 ± 0.4
−10G <sup>cor</sup>	228 ± 165	0.44 ± 0.32	10.9 ± 10.3	4.7 ± 1.1	2.0 ± 0.55	0.24 ± 0.12

<sup>a</sup> Values for  $\tau$ ,  $k_f$ ,  $K_B$ , and  $K_B k_f$  were calculated from tau plots (Figure 4) as outlined in Experimental Procedures. Standard errors were determined from the residuals of the least-squares fit to eq 1. Values of  $k_d$  are the mean ± standard error for the least-squares fit to data from two or more experiments.  $K_{eq} = K_1 K_2 K_3 \cong K_B k_f / k_d$  (7, 23). Data for −10G<sup>cor</sup> are based on values for −10G corrected for incomplete occupancy as outlined in the text.

The reduced occupancy of the −10G mutant promoter that was observed in Figures 1 and 2 is also reflected in steady-state rates of abortive synthesis, which varied between 30 and 50% of the wild-type rate. Incomplete occupancy leads to observed values of  $\tau_{obs}$  that are lower than the actual values and must be corrected by dividing each value of  $\tau_{obs}$  by the fractional occupancy obtained in the lagtime assay. For the two-step mechanism, use of this correction factor can be derived from the treatment of Strickland et al. (22). An elegant treatment of multistep models based on fewer assumptions (23) demonstrated that the same correction factor must be applied even for mechanisms that include additional steps (O. Tsodikoff, personal communication; ref 23). When the data for the −10G promoter were corrected for fractional occupancy (average occupancy in this set of lagtime assays = 0.30, 0.32, and 0.53 at 20, 50, and 100 nM [RNAP], respectively) and then replotted to fit eq 1, the calculated values of the kinetic parameters were  $K_B = 10.9 \pm 10.3 \times 10^6 \text{ M}^{-1}$ ;  $k_f = 0.44 \pm 0.32 \times 10^{-2} \text{ s}^{-1}$ ; and  $K_B k_f = 4.7 \pm 1.1 \times 10^4 \text{ M}^{-1} \text{ s}^{-1}$  (Table 2). Thus, the mutation actually decreases  $k_f$  by a factor of ~20 and  $K_B k_f$  by a factor of ~25. That is, the mutant promoter is substantially weaker than was indicated by the original uncorrected data.

**Determination of Dissociation Rate Constants.** One reason for lower equilibrium levels of  $RP_o$  could be that open complexes are unstable. Therefore, we allowed complexes to form at 37° and then monitored their dissociation in the presence of 30  $\mu\text{g/mL}$  of heparin by assaying samples for activity in abortive initiation experiments. [In 0.1 M glutamate, the dissociation rate for wild-type complexes is essentially constant in the range from 10 to 60  $\mu\text{g/mL}$  of heparin (data not shown), indicating that there is very little, if any, direct attack of heparin at 30  $\mu\text{g/mL}$  on open complexes (see also ref 4).] The observed values of  $k_d$  (Table 2) indicate that complexes formed on all four templates are very stable (half-lives approximately 5–20 h), but that complexes formed at the mutant promoters are approximately 3–5 times less stable than those formed at the wild-type promoters. Thus,  $K_{eq}$ , which equals  $K_B k_f / k_d$  (7, 23), for wild-type  $P_R$  is  $14 \times 10^{10} \text{ M}^{-1}$ , which is about 60 times as great as the corrected value for the −10G promoter mutant (Table 2).

**Interconversion of  $RP_i$  and  $RP_o$ .** Since, at 37 °C, all three mutations affect  $k_f$ , they could in principle affect the third (DNA strand-separation step) in the three-step pathway described by mechanism 2. To investigate the effects of mutations on the equilibrium between  $RP_i$  and  $RP_o$ , we assayed for open complexes by probing with  $\text{KMnO}_4$  following a temperature-shift from 37° to 20°. This is a modified version of experiments of Buc and McClure (6),

who used abortive initiation to follow the reequilibration of  $RP_i$  and  $RP_o$  at the  $lacP_{UV5}$  promoter following a temperature shift. The rationale for these experiments is that immediately preceding the shift, the extent of cleavage at thymidine residues will reflect the number of open complexes ( $RP_o$ ) formed at 37°, but reequilibration between  $RP_i$  and  $RP_o$  at 20° will result in reduced sensitivity to  $\text{KMnO}_4$ . After the shift, there should be three types of stable complexes in rapid equilibrium:  $RP_i$  and two forms of  $RP_o$  (3, 20, 24).  $RP_i$  should be insensitive to  $\text{KMnO}_4$  (3, 20),  $RP_{o2}$  should be fully strand-separated, resulting in  $\text{KMnO}_4$ -induced cleavage at +2, while  $RP_{o1}$  should be partially open, which should be reflected by cleavage at −3 and −4 (Figure 3) but not at +2 (3, 20, 24).

For wild-type and the −10C and −10A mutant promoters, open complexes form on all (or nearly all) templates during the initial incubation, but based on the steady-state rates of abortive synthesis, footprinting data, and gel mobility shift assays (25), this is not the case for the −10G promoter (gel mobility shift data not shown). Therefore, to prevent formation of complexes between free RNAP and DNA following the temperature shift, we performed the temperature-shift experiments in the presence of 30  $\mu\text{g/mL}$  heparin, which prevents RNAP binding to DNA but does not inactivate  $RP_i$  or  $RP_o$  (see above).

A phosphorimager was used to quantify data similar to those illustrated in Figure 3. A clearer distinction between bands reflecting cleavage at −3 and −4 was obtained at lower phosphorimager intensities than are displayed in Figure 3 (see also ref 14). At 37°, the wild-type promoter was expected to yield only fully strand-separated open complexes ( $RP_{o2}$ ) at time zero. However, as in Figure 3, the band representing cleavage at −3 was 2–3 times as intense as the band at +2, not only for the wild-type promoter but for the mutants as well. We interpret this observation to mean that when DNA strands are fully separated, the T at −3 is much more sensitive to cleavage than is the T at +2. A similar result was reported by Tsodikov et al. (20).

In Figure 5, the decay in occupancy of  $RP_o$  is plotted as a function of time relative to the initial intensity of the band at +2. The data were fit to eq 2, yielding values of  $K_3$  and  $\beta$  and fractional occupancies listed in Table 3 (columns 1–3). There is very little difference among the four promoters in the conversion of  $RP_i$  to  $RP_o$ . While there is apparently an increase in  $\beta_{app}$  for two of the mutants (−10C and −10A), determination of the rate of reequilibration is subject to substantial experimental error. In addition, the plateau values indicate that there is no significant difference in  $K_3$ .

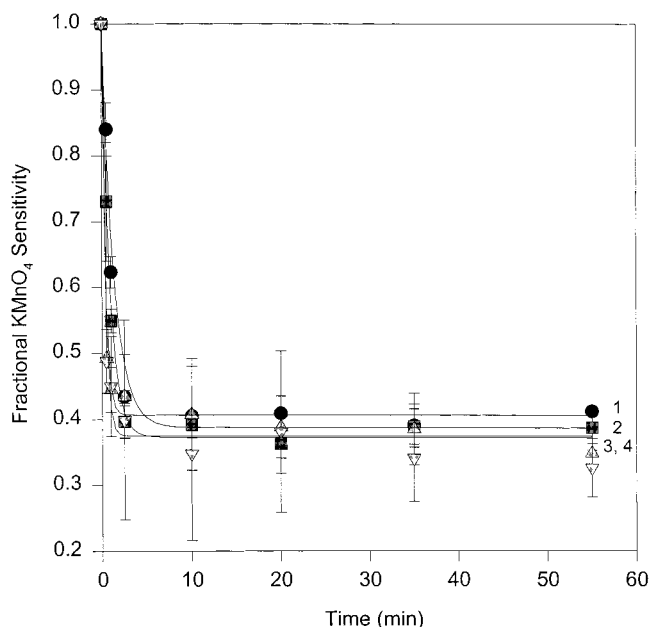


FIGURE 5:  $\text{KMnO}_4$ -sensitivity assays of interconversion of  $\text{RP}_i$  and  $\text{RP}_o$  at 20 °C. At indicated times, samples were withdrawn for treatment with  $\text{KMnO}_4$  as outlined in Experimental Procedures. At each time point, the band corresponding to cleavage at the +2 thymidine residue was quantified using a phosphorimager. After correcting for the amount of radioactivity in the reference band at each time point and normalizing to the value at time zero, the data were fit to eq 2. Each point represents the average of two experiments. The graph in each case represents the theoretical best fit to eq 2. Symbols represent wild-type  $P_R$  (●, curve 1); -10A (■, curve 2); -10C (gray-shaded up triangle, curve 3); -10G (gray-shaded down triangle, curve 4).

The same experiments were assayed by monitoring the decay in intensity of the band at -3 as a function of time at 20°. The data are plotted in Figure 6, this time with 100% reflecting the intensity of the band at -3 at zero time. Fractional occupancy at equilibrium (Table 3, columns 3 and 6) was calculated from the computer-estimated equilibrium constants. If all of the complexes at equilibrium were  $\text{RP}_{o2}$ , fractional occupancies in columns 3 and 6 should be identical. The fact that the fractional sensitivities based on the extent of cleavage at -3 are greater than or equal to the corresponding values based on cleavage at +2 indicates that (as expected) at equilibrium at 20°, some open complexes are  $\text{RP}_{o1}$  (24).

If relative sensitivities of the T's at -3 and +2 are unchanged during the time course of the experiment, the fraction of stable complexes in each state ( $\text{RP}_i$ ,  $\text{RP}_{o1}$ , and  $\text{RP}_{o2}$ ) at equilibrium can be calculated (Table 3, columns 3, 6, 7, and 8). Although the fractional occupancies are not identical for all promoters, differences among them are too small to account for the observed differences in  $k_f$  (Table 2). For the -10A and -10C promoters, there is an apparent deficiency in the total fraction of open complexes (column 6). For these mutants, the plateau values in Figure 6, which reflect total open complex, are not very different from those in Figure 5, which reflect  $\text{RP}_{o2}$ . Thus, there may be a deficiency in  $\text{RP}_{o1}$ . However, considering potential errors in quantification of phosphorimaging data and possible variation in cleavage conditions, the apparent deficiency is probably not significant. (Data for these two mutants were obtained in separate experiments in which the ratio of the intensities

of bands at -3 to those at +2 were about 20% lower than the corresponding ratios in the experiments with the wild-type and -10G promoters.) In any event, calculation of rate constants associated with the formation of  $\text{RP}_i$  from  $\text{RP}_c$  (see next section) indicate that variations in the measured plateau levels and equilibrium constants in Table 3 do not contribute significantly to the overall rate of open complex formation.

**Effects of Mutations on  $k_2$ .** The mutations at -10 all affect  $k_f$ , which reflects the overall rate of conversion of  $\text{RP}_c$  to  $\text{RP}_o$ . In terms of promoter recognition, an important question is whether the mutations affect  $k_f$  primarily through an effect on  $k_3$  and  $k_{-3}$  or through an effect on  $k_2$ . This is equivalent to asking whether the mutations primarily affect DNA unwinding (and recognition of single-stranded DNA) or steps preceding DNA unwinding (including recognition of double-stranded DNA). The relationship between the parameters of the three-step and two-step models is given by the following equations (6, 23):

$$K_B = K_1(k_2 + k_3 + k_{-3})/(k_3 + k_{-3}) \quad (3a)$$

$$1/k_f = 1/k_2 + 1/(k_3 + k_{-3}) = 1/k_2 + 1/\beta \quad (3b)$$

$$k_d = k_{-2}/(1 + K_3) \quad (3c)$$

Note that  $K_B k_f = K_1 k_2$ , and when  $k_2 \ll k_3 + k_{-3}$ ,  $K_B = K_1$ , and  $k_f = k_2$ .

For our purposes, the key question is whether  $1/\beta$  contributes significantly to  $1/k_f$ , the time required for the transition from  $\text{RP}_i$  to  $\text{RP}_o$ . Equation 3b can be used to calculate the times required for each step (Table 4, columns 1–3). In these calculations, we used values of  $\beta$  obtained from assays of  $\text{KMnO}_4$ -sensitivity at -3 (Figure 5), which reflects the total population of open complexes. Values of  $\beta$  were determined at 20°, but the other parameters were measured at 37°. To approximate expected values of  $\beta$ , the measured values have been multiplied by a factor of 15. This corresponds to the predicted change in  $\beta$  for  $\text{lacP}_{UV5}$  over the same temperature range (6). On the basis of this approximation, we conclude that for all three mutants, the rate-limiting step in the isomerization of  $\text{RP}_c$  to  $\text{RP}_o$  is the formation of  $\text{RP}_i$  ( $k_2$ ) and that the predominant effect of the mutations is clearly on  $k_2$ . For the -10G promoter, this conclusion is valid whether corrected or uncorrected values of  $1/k_f$  are used in the calculations but is much more dramatic when the appropriately corrected data are used. For wild-type  $P_R$ , the contribution of  $1/\beta$  to  $1/k_f$  is proportionately greater because the isomerization of  $\text{RP}_c$  to  $\text{RP}_i$  is very fast. Although these calculations depend on extrapolation of values of  $\beta$  obtained at 20° to obtain estimates of the corresponding values at 37°, except in the case of wild-type  $P_R$ , calculations of  $1/k_2$  would hardly be affected if values for  $\beta$  for the mutants were overestimated by a factor of 5.

Table 4 (columns 4–6) presents similar calculations of kinetic parameters at 20°. In this case, since  $\tau$  ( $1/k_f$ ) is measured at 37° (Table 2), estimates of  $\tau$  at 20° were obtained by multiplying values obtained at 37° by a factor of 8. Again, this approximates the change in  $k_f$  for  $\text{lacP}_{UV5}$  over the same temperature range (6). At 20°, the mutations have a major effect on  $k_2$ , but, as expected, the equilibrium between  $\text{RP}_i$  and  $\text{RP}_o$  contributes to a slightly greater extent



Table 3: Determination of  $K_{3,app}$  and  $\beta_{app}$  Based on  $KMnO_4$ -Sensitivity<sup>a</sup>

template	sensitivity of thymidine at +2			sensitivity of thymidine at -3			equilibrium fractions <sup>b</sup>	
	(1) $K_{3(2)}$	(2) $\beta_{(2)}$ (min <sup>-1</sup> )	(3) $f_{e2}$ (RP <sub>o2</sub> /RP <sub>tot</sub> )	(4) $K_{3(-3)}$	(5) $\beta_{(-3)}$ (min <sup>-1</sup> )	(6) $f_{e1,2}$ [(RP <sub>o1</sub> + RP <sub>o2</sub> )/RP <sub>tot</sub> ]	(7) RP <sub>o1</sub> /RP <sub>tot</sub>	(8) RP <sub>i</sub> /RP <sub>tot</sub>
wild-type $P_R$	0.6 ± 0.06	0.7 ± 0.08	0.4 ± 0.05	1.1 ± 0.02	1.6 ± 0.05	0.5 ± 0.02	0.1 ± 0.07	0.5 ± 0.02
$P_R$ (-10A)	0.7 ± 0.02	2.6 ± 0.7	0.4 ± 0.02	0.8 ± 0.04	4.3 ± 1.8	0.4 ± 0.03	0.02 ± 0.05	0.6 ± 0.03
$P_R$ (-10C)	0.6 ± 0.03	2.7 ± 0.6	0.4 ± 0.03	0.7 ± 0.02	3.2 ± 0.6	0.4 ± 0.02	0.01 ± 0.05	0.6 ± 0.02
$P_R$ (-10G)	0.6 ± 0.02	1.1 ± 0.03	0.4 ± 0.02	1.3 ± 0.07	2.5 ± 0.2	0.6 ± 0.05	0.2 ± 0.07	0.4 ± 0.05

<sup>a</sup> Values of  $K_3$  and  $\beta$  (± standard errors) were determined from a computerized best-fit of data in Figures 5 and 6 to eq 2; at equilibrium,  $f_{e2} = K_{3(2)}/(1 + K_{3(2)})$  and  $f_{e1,2} = K_{3(-3)}/(1 + K_{3(-3)})$ . <sup>b</sup> RP<sub>i</sub>/RP<sub>tot</sub> = 1 -  $f_{e1,2}$  (column 7); RP<sub>o1</sub>/RP<sub>tot</sub> =  $f_{e1,2} - f_{e2}$  (column 8). Values of  $K_3$  for the -10G promoter are not corrected for the fraction of RP<sub>i</sub> prior to the temperature shift (see Discussion).

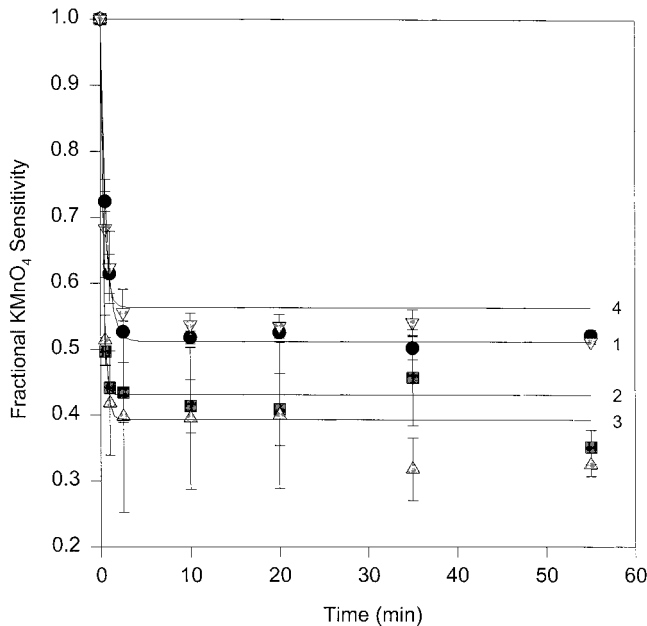


FIGURE 6:  $KMnO_4$ -sensitivity assays of interconversion of RP<sub>i</sub> and RP<sub>o</sub> at 20 °C. Data are from the same experiments as in Figure 5, except that each point is based on quantification of cleavage at the thymidine residue at -3. Symbols are as in Figure 5.

to the time required for open complex formation than it does at 37°.

## DISCUSSION

**Effects of -10 Mutations.** Qualitatively, the kinetic analysis indicates that at position -10 in  $P_R$ , the rank ordering of promoter strength as a function of the sequence in the nontemplate (top) strand is T > C ≈ A > G. This hierarchy is identical to that found in vivo for the *ant* promoter (10).

The kinetics of open complex formation at wild-type  $\lambda$   $P_R$  (and  $lacP_{UV5}$ ) as a function of temperature, salt concentration, and presence of divalent cations have been well-studied (1, 4–6, 21). For wild-type  $P_R$ , experimental data (3–5, 20) provide substantial support for the three-step mechanism, which has been thoroughly analyzed theoretically (23). However, the effects of single base pair substitutions on kinetic parameters characterizing the three-step pathway have not been fully analyzed for any promoter. Historically, it was suspected that information required for the two-step pathway to the open complex was partitioned between the two consensus regions (-35, TTGACA, and -10, TATAAT) for  $\sigma^{70}$ -containing *Escherichia coli* RNAP (26). Despite initial evidence in favor of such partitioning,

it is now known that mutations in the -35 region can affect either  $K_B$  or  $k_f$  or both (11, 27–29). However, all -10 region mutations for which kinetic data have been published affect only  $k_f$  (28, 29). While the original hypothesis was that mutations in the -10 region would directly affect DNA strand separation per se, the kinetic analysis (Tables 2–4) indicates that the primary effect of the mutations at -10 in  $P_R$  is on the isomerization of RP<sub>c</sub> to RP<sub>i</sub>, which is thought to involve both a conformational change in RNAP (3, 7) and DNA untwisting (30).

Thus, at 37°, DNA strand-separation at wild-type  $P_R$  is not rate-limiting (2, 3), and extrapolation of values of  $\beta$  from 20 to 37° indicate that it is not rate-limiting for the mutants. The data in Table 3 also indicate that the mutations do not substantially affect the transition from RP<sub>i</sub> to RP<sub>o</sub> even at 20°, when a significant fraction of the complexes at equilibrium are RP<sub>i</sub>.

Evidence that the mutations do not affect strand-separation per se comes primarily from experimentally determined values of  $K_3$  at 20°. However, calculations of  $k_2$  at 37° based on extrapolated values of  $\beta$  (Table 4) are consistent with this conclusion. The extrapolation was based on the assumption that the temperature-dependence of kinetic parameters for  $P_R$  would be similar to that of the corresponding parameters for  $lacP_{UV5}$ . The validity of this assumption is supported qualitatively by data from the Record laboratory (2, 3, 7, 20), although the temperature-dependence of  $\beta$  has not been measured directly. Nevertheless, the estimates of  $\beta$  obtained by extrapolation could be subject to substantial error without significantly affecting the calculated values of  $k_2$ . In addition, the extrapolation was performed by multiplying the 20° values of  $\beta$  by a factor of 15, which is actually a low estimate of the corresponding factor for  $lacP_{UV5}$  (6). Thus, the extrapolation yielded values for  $1/\beta$ , the time required for equilibration of RP<sub>i</sub> and RP<sub>o</sub>, that are likely to be overestimates (and thus exaggerate the potential effect of this step on  $k_f$ ).

Finally, because complexes detectible by gel mobility shift assays are very stable at 20° (half-times ~10 h, data not shown), the mutations must decrease the forward rate constant  $k_2$  in the three-step mechanism (see eq 3c).

**Isomerization of RP<sub>i</sub> to RP<sub>o</sub>.** Equation 2 (6) is based on models that include only one form of open complex. When both RP<sub>o1</sub> and RP<sub>o2</sub> (24) are taken into account, the transition from RP<sub>i</sub> to RP<sub>o2</sub> yields an equation for the time course of reequilibration of RP<sub>i</sub> and RP<sub>o2</sub> that has the same form as that of eq 2, but  $K_3$  and  $\beta$  are more complicated functions of the equilibrium and rate constants associated with a two-step isomerization than simply  $K_3$  and  $\beta$  ( $= k_3 + k_{-3}$ ). However, since RP<sub>o1</sub> and RP<sub>o2</sub> are in rapid equilibrium, the

Table 4: Time Required for Isomerization from  $RP_c$  to  $RP_i^a$ 

	(1)	(2)	(3)	(4)	(5)	(6)
$P_R$	$\tau$	$1/\beta$	$1/k_2$	$\tau$	$1/\beta$	$1/k_2$
allele	37°	37°	37°	20°	20°	20°
w.t. (−10T)	11 ± 6	2.5 ± 0.1	8.5 ± 6	88 ± 48	38 ± 1.2	50 ± 49
−10C	32 ± 5	0.9 ± 0.4	31 ± 6	260 ± 40	14 ± 6.0	240 ± 50
−10A	46 ± 23	1.3 ± 0.2	45 ± 23	370 ± 180	19 ± 3.3	320 ± 210
−10G	88 ± 32	1.6 ± 0.1	86 ± 32	700 ± 24	24 ± 2.0	620 ± 30
−10G <sup>cor</sup>	230 ± 170	1.6 ± 0.1	230 ± 170	1800 ± 1300	24 ± 2.0	1800 ± 1300

<sup>a</sup> All of the data are expressed in seconds.  $\tau = 1/k_t$  at 37° is based on tau plots (Figure 3); values of  $\tau$  at 20° are based on extrapolation of data for  $lacP_{UV5}$  (6).  $1/\beta$  at 20° was determined in temperature-shift experiments (Table 3; Figure 5); values of  $1/\beta$  at 37° are based on extrapolation of data for  $lacP_{UV5}$  (6). Values of  $1/k_2$  were calculated using eq 3b. Data for −10G<sup>cor</sup> are based on values for −10G corrected for incomplete occupancy as outlined in the text.

apparent constants should be a close approximation to the actual constants (14, 23).

The foundation for these experiments, especially the use of temperature shifts, is based in part on the observation that two different methods of measuring the fraction of  $lacP_{UV5}$  open complexes yielded nearly identical results at several different temperatures between 14 and 25 °C (6). One of the methods involved downshifts to several different temperatures, while the other involved continuous incubation at the same temperatures. For  $\lambda P_R$ , thermodynamic and structural analyses of complexes formed at various temperatures or after a shift to 0° yielded results consistent with formation of the same kinetic intermediates at each temperature (3–5, 20, 23). The more recent mathematical treatment of the three-step model based on experimental data obtained for  $P_R$  wild-type provides further support for the kinetic analysis (23). Although there could be small variations in structure among kinetically equivalent intermediates, especially in the region in which strand separation occurs (18), such differences would not alter the kinetic analyses (23) on which the conclusions presented here are based.

For all of the mutants, complexes formed at 37° and then shifted to 20° reequilibrated very rapidly (Figures 5 and 6) in comparison to their dissociation rate. These results support the assumptions on which the determination of  $K_3$  were based and the conclusion that the mutations primarily affect step(s) in open complex formation prior to DNA strand separation per se.

Nevertheless, one difference between the −10G mutant and the wild-type promoter suggests a possible effect of the mutation on  $K_3$  at 37°. The estimated maximal occupancy of the mutant promoter based on DNase I footprinting is ~75% (Figure 2), but the estimated occupancy based on KMnO<sub>4</sub>-sensitivity (Figure 3) is ~66%. These data indicate that 10–15% of the stable complexes formed at the −10G promoter are  $RP_i$ . In a direct comparison of stable complex formation with steady-state rates of abortive synthesis, relative occupancy of the mutant template measured in gel mobility shift assays (data not shown) was again approximately 75%, but ~20–25% of the complexes formed were inactive in abortive initiation. [For the sake of argument, it is assumed that all the “non-productive” complexes at 37° are  $RP_i$  and none are  $RP_{oi}$  or inactive for some other reason.] Thus, at 37°, estimates of  $K_3$  for the mutant promoter range between 3.5 (20–25%  $RP_i$ ) and 8 (10–15%  $RP_i$ ), which differs substantially from the wild-type  $K_3$  (see next section and ref 3).

If, at time zero, just prior to a temperature shift (Figures 5 and 6), only 75–80% of the stable complexes are  $RP_o$ ,

then the actual fraction of open complexes after reequilibration must be 75–80% of the observed fraction. Thus, for −10G, the fraction of open complexes at equilibrium at 20° (based on cleavage at −3) should be 0.40–0.42 rather than 0.56 and the actual value of  $K_3$  should be about 0.7 instead of 1.3. Neither the corrected nor uncorrected value of the equilibrium constant is significantly different from the wild-type value (1.1).

Thus, a mutation from T:A to G:C, which should stabilize the DNA double-helix in the region in which strand separation occurs, appears to inhibit DNA strand separation. However, this difference must be based on nucleotide sequence and not just the stability of the double helix, since −10C a change from T:A to C:G does not detectably alter  $K_3$  at 37°.

**Effects of  $K_3$  on  $k_d$ .** Equation 3b predicts that a change in  $K_3$  should affect  $k_d$ . If, for example, at 37°, 96% of the stable complexes at the wild-type promoter were  $RP_i$ , but only 90% were  $RP_i$  at a mutant promoter,  $k_d$  would be reduced by a factor of 2.5. These differences in levels of  $RP_i$  would be undetectable experimentally but could account for observed decreases in  $k_d$  for any of the mutant promoters. For the −10G promoter, one might expect an even greater decrease in  $k_d$ , but given imprecision in the measurements of half-lives of very stable complexes and in determining the fraction of  $RP_i$  for the wild-type promoter, the measurements of  $K_3$  and  $k_d$  are consistent within the limitations of the experiments. On the basis of eq 3c and the data in Tables 2 and 3, it is possible that a small fraction (perhaps ~4%) of stable complexes at the wild-type promoter at 37° are  $RP_i$ . That is,  $K_3$  for the wild-type promoter appears to be ~25.

**Reduced Occupancy of the −10G Mutant Promoter.** In the three-step mechanism  $K_{eq} (K_1 K_2 K_3)$  for the formation of open complexes is given by  $K_{Bkf}/k_d$  (6, 7, 23). For −10G, the corrected value of  $K_{eq}$ ,  $0.2 \times 10^{10} \text{ M}^{-1}$ , yields an estimated occupancy at 20 nM RNAP of 76%, based on eq 10 of Tsodikov and Record (23) and a value of  $K_3$  of 3.5 for the mutant promoter. Although this calculated reduction in occupancy of  $RP_o$  is not so great as the observed reduction (roughly about 50%, depending on the experiment), there is substantial experimental error in the corrected value of  $K_{Bkf}$  and in measurements of  $k_d$ . What is most notable is that the equilibrium constant for the wild-type  $P_R$  is about 60 times the value for the mutant promoter.

Previously, we considered the possibility that incomplete occupancy could reflect the formation of binary complexes at an overlapping promoter (14). Such complexes would have to exclude (compete with) open complex formation at  $P_R$ ,



be inactive in abortive initiation assays (or require substrates other than CpA and UTP), and be undetectable in gel retardation or DNase I footprinting assays. The existence of a competing promoter with these properties seems unlikely.

In the previous study (14), we observed 60% occupancy of a  $P_R$  mutant with a single bp deletion between the  $-10$  and  $-35$  consensus regions (14). Interestingly, the corrected values of  $K_{\text{B}}k_{\text{f}}$  ( $7.2 \times 10^4 \text{ M}^{-1} \text{ s}^{-1}$ ) and  $K_{\text{eq}}$  ( $2.1 \times 10^9 \text{ M}^{-1}$ ) for the deletion mutant are very similar to the values obtained for the  $-10\text{G}$  promoter. This should not be surprising since incomplete occupancy will, in any case, be a property of relatively weak promoters.

## ACKNOWLEDGMENT

We thank Fyodor Tereshchenko for purified RNAP and Dr. Oleg Tsodikov for helpful discussions. This work was supported in part by NIH Grant GM50577.

## REFERENCES

- McClure, W. R. (1985) *Annu. Rev. Biochem.* 54, 171–204.
- Record, M. T., Jr., Reznikoff, W. S., Craig, M. L., McQuade, K. L., and Schlax, P. J. (1996) in *Escherichia coli and Salmonella typhimurium: Cellular and Molecular Biology* (Neidhardt, F. C., Ed.) 2nd ed., pp 792–820, ASM Press, Washington, DC.
- Craig, M. L., Tsodikov, O. V., McQuade, K. L., Schlax, P. E., Jr., Capp, M. W., Saecker, R. M., and Record, M. T., Jr. (1998) *J. Mol. Biol.* 283, 741–756.
- Roe, J.-H., Burgess, R. R., and Record, M. T., Jr. (1984) *J. Mol. Biol.* 176, 495–521.
- Roe, J.-H., Burgess, R. R., and Record, M. T., Jr. (1985) *J. Mol. Biol.* 184, 441–453.
- Buc, H., and McClure, W. R. (1985) *Biochemistry* 24, 2712–2723.
- Leirmo, S., and Record, M. T., Jr. (1990) *Nucleic Acids Mol. Biol.* 4, 123–151.
- Roberts, C., and Roberts, J. W. (1996) *Cell* 86, 495–501.
- Marr, M., and Roberts, J. W. (1997) *Science* 276, 1258–1260.
- Moyle, H., Waldburger, C., and Susskind, M. M. (1991) *J. Bacteriol.* 173, 1944–1950.
- Woody, S. T., Fong, R. S.-C., and Gussin, G. N. (1993) *J. Mol. Biol.* 229, 37–51.
- Fong, R. S.-C., Woody, S., and Gussin, G. N. (1994) *J. Mol. Biol.* 240, 119–126.
- McClure, W. R. (1980) *Proc. Natl. Acad. Sci. U.S.A.* 77, 5634–5638.
- McKane, M., and Gussin, G. N. (2000) *J. Mol. Biol.* 299, 337–349.
- Burgess, R. R., and Jendrisak, J. J. (1975) *Biochemistry* 14, 4634–4638.
- Lowe, P., Hager, D. A., and Burgess, R. R. (1979) *Biochemistry* 18, 1344–1352.
- Cech, C. L., and McClure, W. R. (1980) *Biochemistry* 19, 2440–2447.
- Helmann, J. D., and deHaseth, P. L. (1999) *Biochemistry* 38, 5959–5967.
- Sasse-Dwight, S., and Gralla, J. D. (1989) *J. Biol. Chem.* 264, 8074–8081.
- Tsodikov, O. V., Craig, M. L., Saecker, R. M., and Record, M. T., Jr. (1998) *J. Mol. Biol.* 283, 757–759.
- Leirmo, S., Harrison, C., Cayley, D. S., Burgess, R. R., and Record, M. T., Jr. (1987) *Biochemistry* 26, 2095–2101.
- Strickland, S., Palmer, G., and Massey, M. (1975) *J. Biol. Chem.* 250, 4048–4052.
- Tsodikov, O. V., and Record, M. T., Jr. (1999) *Biophys. J.* 76, 1320–1329.
- Suh, W. C., Ross, W., and Record, M. T., Jr. (1993) *Science* 259, 358–361.
- Straney, S. B., and Crothers, D. M. (1987) *Biochemistry* 26, 5063–5070.
- Gilbert, W. (1976) in *RNA Polymerase* (Losick, R., and Chamberlin, M., Eds.) pp 193–205, Cold Spring Harbor Laboratory, Cold Spring Harbor, NY.
- Hawley, D. K., and McClure, W. R. (1982) *J. Mol. Biol.* 157, 493–525.
- Shih, M.-C., and Gussin, G. N. (1983) *Proc. Nat. Acad. Sci. U.S.A.* 80, 496–500.
- Shih, M.-C., and Gussin, G. N. (1983) *Cell* 34, 941–949.
- deHaseth, P. L., and Helmann, J. D. (1995) *Mol. Microbiol.* 16, 817–824.

BI0019085